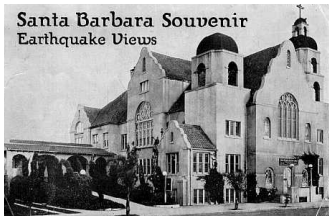

4th IASPEI / IAEE International Symposium:

Effects of Surface Geology on Seismic Motion

August 23–26, 2011 · University of California Santa Barbara

NONLINEARITY IN SITE RESPONSE -NONLINEAR VOLUMETRIC MECHANISM

Susumu Iai
Disaster Prevention Research Institute
Kyoto University
Uji, Kyoto 611-0011
Japana

Tetsuo Tobita
Disaster Prevention Research Institute
Kyoto University
Uji, Kyoto 611-0011
Japan

Tomotaka Iwata
Disaster Prevention Research Institute
Kyoto University
Uji, Kyoto 611-0011
Japan

ABSTRACT

Dry soil tends to resist isotropic compressive stress because contact forces between soil particles are mobilized during compression. However, when the dry soil is subject to tension, volumetric stretching (expansive) strain will be mobilized and eventually soil particles will lose contacts among themselves with no isotropic stress mobilized in the soil. In the field, gravity provides static compression stress in the soil. When subjected to a vertical motion, the confining pressure may increase or decrease depending on the change in volumetric strain induced by the vertical motion. When the motion is small, the mechanism may be approximated by a linear volumetric mechanism. However, when the motion becomes sufficiently large, the change in the confining pressure will cause volumetric strain beyond the limit where there will be no compressible stress. In this manner, the dry soil can exhibit nonlinear volumetric mechanism during earthquakes. The analysis of the asymmetric vertical motion with a peak acceleration of 4.0g recorded during the 2008 Iwate-Miyagi Inland, Japan, earthquake suggests that this type of nonlinearity in site response can result in significantly high peak acceleration in vertical motion.

INTRODUCTION

When a medium dense or firm ground is subject to moderate earthquake motions, soil behaves like linear material with reduced shear modulus and increased damping factor (Seed and Idriss, 1970; Zeghal et al., 1995; Yoshida and Iai, 1998). In these cases of mild non-linearity that is associated with the strain level in the order of magnitude less than about one percent, equivalent linear model has been often used in research and practice of seismic hazard analysis (Sugito et al., 1994; Dobry and Iai, 2000; NEHRP, 1997; Schnabel et al., 1972). However, when the ground is loose or soft or when the ground undergoes strong earthquake motions, soil non-linearity becomes predominant and soil does not behave like linear or equivalent linear material. The strain level associated with this behavior is in the order of magnitude one percent or larger. As expected, the non-linear behavior of soil is closely related with failure mechanism of soil.

In the previous paper (Iai and Tobita, 2006), an overview on the nonlinearity due to shear mechanism, including liquefaction and cyclic mobility, was presented. In this paper, the nonlinearity due to volumetric mechanism will be presented.

FORMULATION

Isotropic linear elastic material, which plays a central role in seismology and soil dynamics with mild non-linearity, can be described by a linear relationship between the stress tensor $\boldsymbol{\sigma}$ (extension positive) and the strain tensor $\boldsymbol{\varepsilon}$ (extension positive), using the second order identity tensor $\mathbf{I}$, and can be expressed as

$$\boldsymbol{\sigma}\mathbf{I} = -q\boldsymbol{p} + \qquad (1)$$

Using bulk modulus $K = \lambda + (2/3)\mu$ and shear modulus $G = \mu$ with the double dot symbol denoting double contraction where λ and μ are Lame constants , the hydrostatic (compression positive) and deviator components of stresses are given by

$$p = -K\mathbf{I}\varepsilon q\varepsilon\mathbf{I} \quad \varepsilon = \mathbf{I}2G\left(\quad -\frac{1}{3} \otimes \quad : \quad \right) \tag{2}$$

In the equivalent linear model, the shear modulus G, which can be generalized as a complex number to incorporate hysteretic damping, is modified as a function of the shear strain amplitude. However, the material remains isotropic.

The non-linearity in soil originates from two sources: the non-reversible stress strain behavior induced by the partial or total failure of the material and the effect of pore water. Soil is an assembly of soil particles that form a porous structure called the soil skeleton. The pores in the soil skeleton are filled with water if the soil is below the ground water table. In the discipline of soil mechanics (Terzaghi, 1943), the total stress $\boldsymbol{\sigma}$, which acts upon an arbitrary plane within the soil, is partitioned into effective stress $\boldsymbol{\sigma}'$, which is carried by the soil skeleton, and the pore water pressure u (compression positive) (Fig. 1) as

$$\sigma\sigma = \mathbf{I} \quad ' - u \tag{3}$$

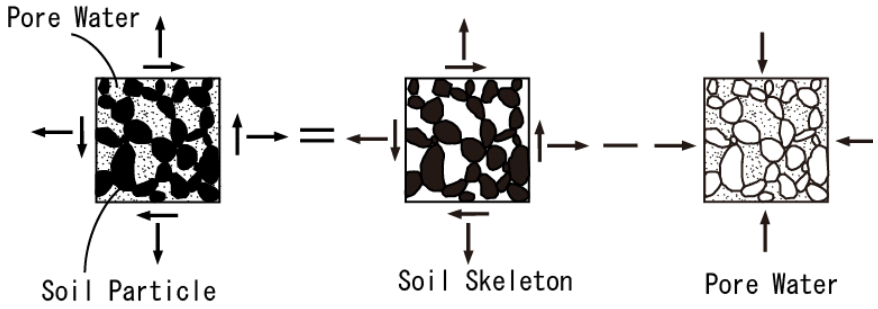

Fig. 1 Schematic figure for total stress, effective stress, and pore water pressure

The overall equilibrium equation of soil is satisfied for total stress $\boldsymbol{\sigma}$, but the deformation of soil is governed by the non-linear relation between effective stress $\boldsymbol{\sigma}'$ and strain $\boldsymbol{\varepsilon}$. In the mechanics of granular materials, stress in granular materials, which are defined as a continuum, is given by a certain average of contact forces between the particles. In a spherical particle assembly, the contact force $\mathbf{P}$ can be partitioned into the direction of contact normal (or along the branch connecting the particle centers) $\mathbf{n}$ and tangential direction $\mathbf{t}$ as (Fig. 2)

$$\mathbf{P} = F\mathbf{n} + S\mathbf{t} \tag{4}$$

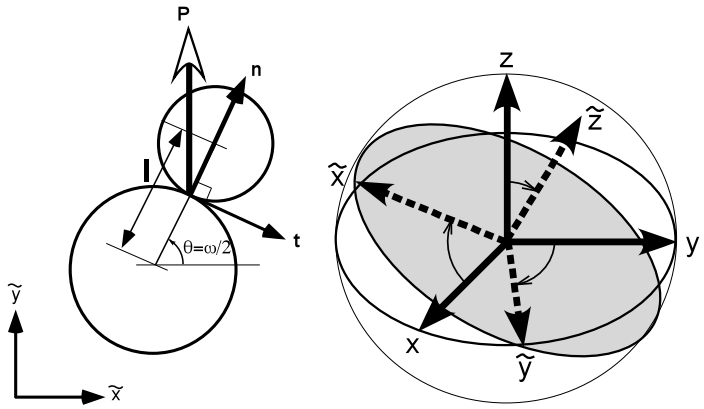

Fig. 2 Contact normal $\mathbf{n}$*, tangential direction* $\mathbf{t}$ *and contact force* $\mathbf{P}$ *defined at particle contact (left) and local co-ordinate* $\tilde{\mathbf{x}}, \tilde{\mathbf{y}}, \tilde{\mathbf{z}}$ *for defining the virtual two dimensional mechanisms (right)*

Taking the average over the contact forces within the representative volume elements with volume V (Oda, 1974; Oda et al., 1985), the macroscopic stress can be expressed as

$$\boldsymbol{\sigma} = \frac{1}{V}\sum l\left(F\,\mathbf{n}\otimes \quad + S\otimes \quad\right) \tag{5}$$

where l denotes length of the branch.

Prior to determining the average of all the contacts with a random orientation, a structure can be identified by systematically grouping the contacts according to their orientation. As depicted in Fig. 2, the first level of structures is identified by choosing pairs of contact force and contact normal that are parallel to the plane specified by the local co-ordinates $\tilde{\mathbf{x}}, \tilde{\mathbf{y}}, \tilde{\mathbf{z}}$ where $\tilde{\mathbf{z}}$ is the axis normal to the plane. Assembling those pairs on the plane constitutes a virtual two-dimensional mechanism. The direction $\mathbf{n}$ within the plane is measured relative to the local coordinate $\tilde{\mathbf{x}}$ with angle $\omega/2$. The average of these two-dimensional mechanisms over the surface of a unit sphere with respect to solid angle Ω defines the macroscopic stress.

Systematically sorting the isotropic and deviator components of the second order tensors in Eq. (5) and using the number of summation to infinity, Eq. (5) can be rewritten as (Iai, 1993)

$$\boldsymbol{\sigma} = -p\,\mathbf{I} + \frac{1}{4\pi}\int\int\left(q_F\mathbf{n}\left\langle \quad\otimes\quad\right\rangle\mathbf{t} + q_S\mathbf{n}\left\langle \quad\otimes\quad\right\rangle\right)\mathrm{d}\omega\mathrm{d}\Omega \tag{6}$$

$$\left\langle \mathbf{n}\otimes\mathbf{n}\right\rangle = \mathbf{n}\otimes\mathbf{n} - \mathbf{t}\otimes\mathbf{t},\quad \left\langle \mathbf{t}\otimes\mathbf{n}\right\rangle = \mathbf{t}\otimes\mathbf{n} + \mathbf{n}\otimes\mathbf{t} \tag{7}$$

where p denotes the effective confining pressure (compression positive), and q_F, q_S denote micromechanical stress contributions to macroscopic deviator stress due to normal and tangential components of contact forces, respectively.

Equation (6) represents the mechanisms with a combination of biaxial shear $\left\langle \mathbf{n}\otimes\mathbf{n}\right\rangle$ and simple shear $\left\langle \mathbf{t}\otimes\mathbf{n}\right\rangle$. However, once these mechanisms are idealized in terms of the second order tensors, they become indistinguishable, except for the difference in the orientation with an angle of $\pi/4$ in terms of $\omega/2$. Thus, Eq. (6) can be rewritten as

$$\boldsymbol{\sigma} = -p\,\mathbf{I} + \frac{1}{4\pi}\int\int q_F\left\langle \quad\otimes\quad\right\rangle\mathrm{d}\omega\mathrm{d}\Omega \tag{8}$$

The direct stress strain relationship is derived by relating macroscopic strain tensor $\boldsymbol{\varepsilon}$ to macroscopic effective stress $\boldsymbol{\sigma}'$ through the structure defined by Eq. (8). By defining the volumetric strain ε (extension positive), the virtual simple shear strain γ, and effective volumetric strain ε' to consider the effect of the volumetric strain due to dilatancy ε_{d} as

$$\varepsilon = \mathbf{I}\boldsymbol{\varepsilon}\mathbf{t},\ \gamma\mathbf{n} = \left\langle \quad\otimes\quad\right\rangle : \quad,\quad \varepsilon' = \varepsilon - \varepsilon_{\mathrm{d}}, \tag{9}$$

then isotropic stress p (compression positive) and virtual simple shear stress q in Eq. (8) are defined through path dependent functions as

$$\mathrm{d}p = -K_{\mathrm{L/U}}\mathrm{d}\varepsilon',\quad \mathrm{d}q = G_{\mathrm{L/U}}\mathrm{d}\gamma \tag{10}$$

where the subscripts L and U respectively denote loading and unloading, which are determined in accordance with the signs of $\mathrm{d}\varepsilon'$ and $\mathrm{d}\gamma$ for volumetric and virtual simple shear mechanisms. Using Eqs. (9) and (10), the incremental form of the constitutive equation is given as

$$\mathrm{d}\boldsymbol{\sigma} = \mathbf{C}\mathrm{d}\boldsymbol{\varepsilon} \quad : \mathrm{d}\ ' \tag{11}$$

$$\mathbf{C} = K_{\mathrm{L/U}}\mathbf{I}\otimes\mathbf{I} + \frac{1}{4\pi}\int\int G_{\mathrm{L/U}}\left\langle \mathbf{t}\otimes\mathbf{n}\right\rangle\otimes\left\langle \mathbf{t}\otimes\mathbf{n}\right\rangle\mathrm{d}\omega\mathrm{d}\Omega \tag{12}$$

$$d\varepsilon_{ij} = d\varepsilon_{ij} - \frac{1}{3} d\varepsilon_{d} \delta_{ij} \tag{13}$$

Although soil non-linearity is complex, its formulation has similarities with isotropic linear elastic material. This can be understood by comparing Eqs. (1) and (2) (linear isotropic materials) to Eqs. (11) and (13) (non-linear granular materials). However, differences are also recognized; soil non-linearity is essentially anisotropic (i.e. direction dependent), and merely adjusting the elastic shear modulus G in Eq.(2) cannot approximate the anisotropy.

NONLINEAR VOLUMETRIC MECHANISM: FORMULATION

Whereas the virtual simple shear mechanism as defined for $G_{\mathrm{L/U}}$ in Eq. (12) is formulated by a hyperbolic relation under a constant confining stress (Iai and Tobita, 2006), the volumetric mechanism as defined for $K_{\mathrm{L/U}}$ in Eq. (12) is formulated as a nonlinear elastic material (by neglecting the difference between the loading and unloading condition indicated by the subscripts L/U) as

$$K_{\mathrm{L/U}} = K_{\mathrm{a}} \left(\frac{p}{p_{\mathrm{a}}} \right)^{n_K} \quad \text{for} \, p \geq 0 \text{ (compression)} \tag{14}$$

Integrated form of Eq. (14) is given, for $n_K \neq 1$, with the condition that $p = 0$ at $\varepsilon' = 0$, as

$$p = \begin{cases} p_{\mathrm{a}} \left(-\left(1 - n_K\right) \dfrac{\varepsilon'}{\varepsilon_{\mathrm{ma}}} \right)^{\frac{1}{1-n_K}} & \text{for } \varepsilon' < 0 \text{ (compression)} \\ 0 & \text{for } \varepsilon' \geq 0 \text{ (extension)} \end{cases} \tag{15}$$

where

$$\varepsilon_{\mathrm{ma}} = \frac{p_{\mathrm{a}}}{K_{\mathrm{a}}} \tag{16}$$

With the typical parameters for sand as $n_K = 0.5$, $K_{\mathrm{a}} = 220300\mathrm{kPa}$ at $p_{\mathrm{a}} = 98\mathrm{kPa}$, the stress strain relationship for volumetric mechanism given by Eq. (15) results in the relationship shown in Fig. 3. Not shown in this figure because of its obviousness is the portion for extension side (on the left side of the figure) where the pressure remains at $p = 0$ for $\varepsilon' > 0$. In the extension side, the tangential shear stiffness also vanishes (i.e. $G_{\mathrm{L/U}} = 0$ for $\varepsilon' > 0$). As shown in Fig. 3, the stress strain curve for volumetric mechanism is a hard spring type for compression side.

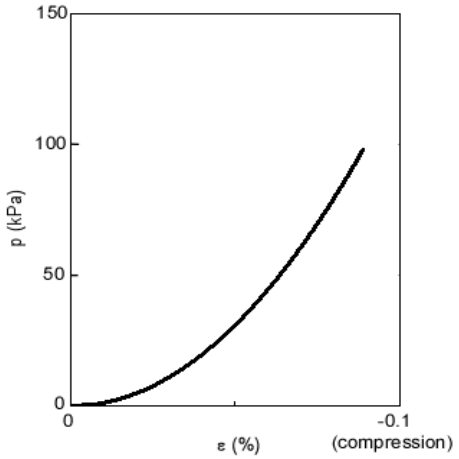

Fig. 3 Drained behavior during isotropic compression

MODEL BEHAVIOR UNDER CYCLIC VERTICAL STRECHING AND COMPRESSION

Behavior of the multiple mechanism model described earlier is investigated by applying vertical compression and tension to a single element (Tobita et al., 2010). The model parameters for this particular study are: $K_a = 605\text{Mpa}$ for $p_a = 49\text{kPa}$, Poisson's ratio=0.33, internal friction angle=35^0 and density of 1.8t/m^3. First, the element is isotropically consolidated with a confining pressure of 49kPa, which is equivalent to the confining stress at a shallow depth about 2.8m in a soil deposit. Then, it is stretched and compressed vertically under drained condition (as for dry soil) by enforcing dynamic cyclic vertical force with 1Hz as shown in Fig. 4, where the horizontal displacements of nodes 3 and 4 are constrained. The stress-strain history shown in Fig. 5 starts at the point "1", where the mean stress is -49kPa, then it is gradually stretched, and once the mean stress reaches zero at "2", volumetric strain abruptly increases up to about 0.3%. On the compression side, the stress-strain follows the curve whose initial tangential slope is defined by the rebound modulus of K=605MPa.

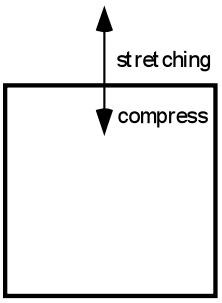

Fig.4 Schematic figure for normal stretching/compression of soil element

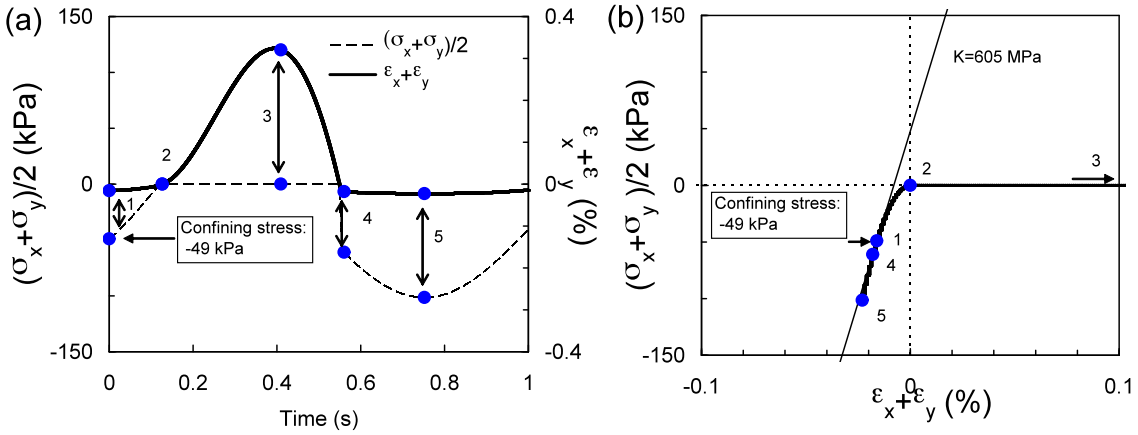

Fig. 5 Stress strain behavior during normal cyclic stretching/compression (a) time histories, (b) stress strain relationship

MODEL BEHAVIOR UNDER CYCLIC VERTICAL INPUT ACCELERATION

In order to discuss the fundamental effect of soil non-linearity on seismic site response, an idealized uniform sand deposit 10m thick was considered for analysis. In the previous study (Iai and Tobita, 2006), this deposit was subject to a horizontal sinusoidal input acceleration to evaluate the non-linear effects due to shear mechanism, including liquefaction and cyclic mobility. In this study, the deposit was subject to the cyclic vertical input acceleration with 10Hz under the drained (dry) condition. The same soil parameters as shown earlier were used. In the analysis, the deposit was first subject to a gravity field of 1g. The gravity induces the initial confining stress varying with a depth in the soil deposit. Next, the deposit was subject to the cyclic vertical input acceleration and dynamic response of the deposit was computed. The dynamic analysis was performed in the gravitational field.

The amplitude of the vertical input acceleration used from the analysis ranges from 0.5g (=4.9m/s^2) to 2g (=19.6m/s^2). The results are shown in Figs. 6 through 8 where the volumetric stress and strain are computed near ground surface (at a depth of 0.25m from the ground surface). The ground surface acceleration shows an asymmetric time history as shown in these figures with a higher peak acceleration in upward direction. As the amplitude of the input acceleration increases, the asymmetry becomes more pronounced and resulted in the spike like motion at the amplitude of 2g. The spike occurs when the soil is compressed from the stretching regime. As shown in Fig. 8(c), soil can go into a stretching regime with no confining stress when subject to a large vertical acceleration. The spike occurs when the soil follows the stress path for compression side of the stress strain curve having a hard spring type. As shown in Figs. 6 through 9, concentration of acceleration in terms of response amplitude and duration occurs as a consequence of nonlinear response when subject to a material having a mechanical property with a hard spring type.

In the analysis, the entire soil deposit of 10m was instantaneously underwent the stretching regime 1g and 2g input motion. For 2g input motion, the entire soil deposit of 10m was repetitively underwent into stretching regime. For 1g input motion, only at the shallower depth of 4m was subject to the repetitive stretching regime.

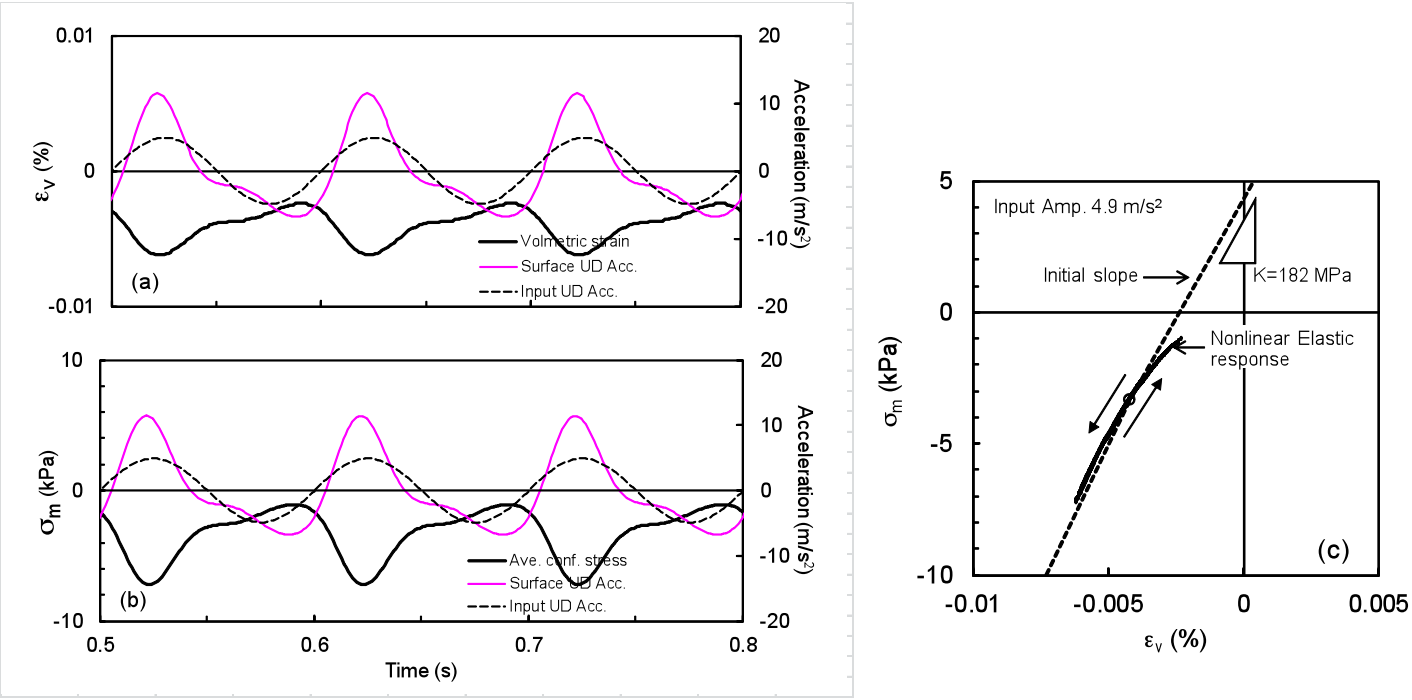

Fig. 6 Response of idealized soil deposit under vertical input acceleration with an amplitude of 0.5g(=4.9m/s^2); (a) surface and input acceleration and volumetric strain near ground surface, (b) mean stress with accelerations, (c) stress strain response for volumetric mechanism near ground surface

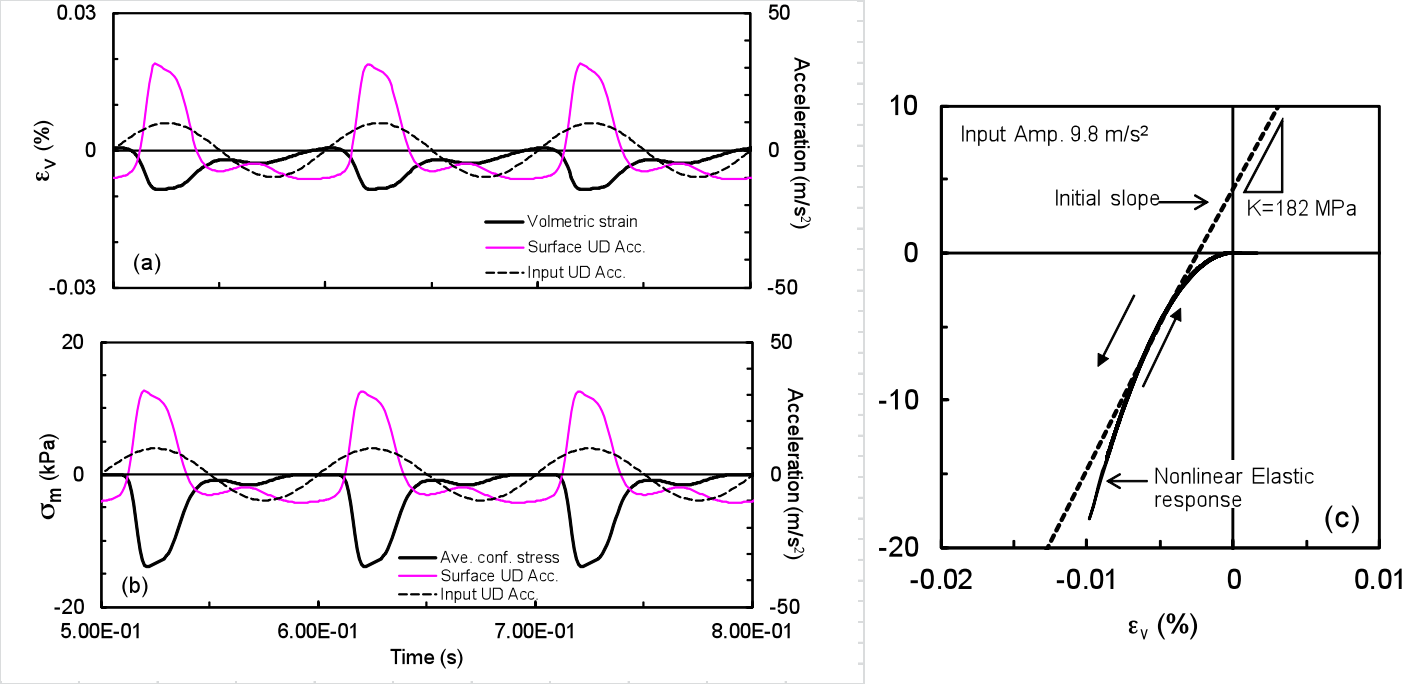

Fig. 7 Response of idealized soil deposit under vertical input acceleration with an amplitude of 1.0g(=9.8m/s^2); (a) surface and input acceleration and volumetric strain near ground surface, (b) mean stress with accelerations, (c) stress strain response for volumetric mechanism near ground surface

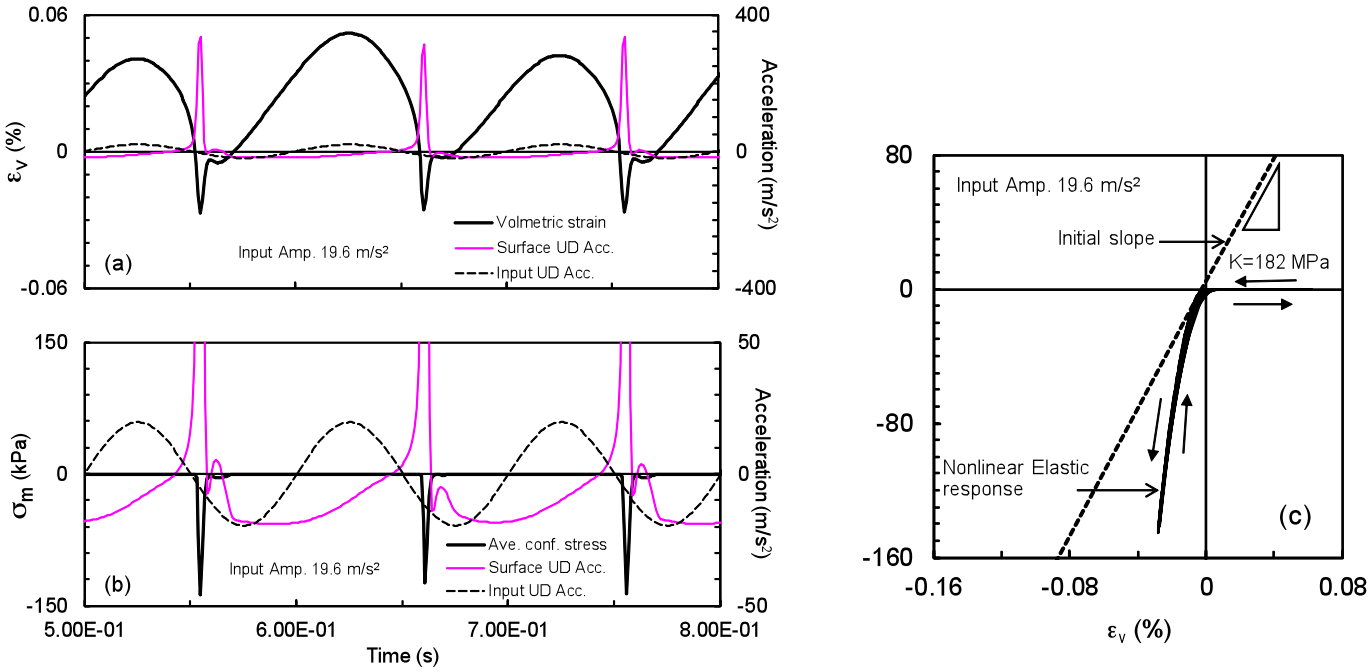

Fig. 8 Response of idealized soil deposit under vertical input acceleration with an amplitude of 2.0g(=19.6m/s^2); (a) surface and input acceleration and volumetric strain near ground surface, (b) mean stress with magnified plot for acceleration, (c) stress strain response for volumetric mechanism near ground surface

NONLINEAR VOLUMETRIC MECHANSM: EVIDENCE FROM THE FIELD

An asymmetric vertical acceleration record was obtained at Ichinoseki-west KiK-net IWTH25 station, Japan, during the 2008 Iwate-Miyagi inland, Japan, earthquake (magnitude M=7.2, depth 8.0km)with a peak ground acceleration of 4g in vertical component (Aoi et al., 2008). The measured time histories at the ground surface and at a depth of 260m are shown in the second and the third rows in Fig. 9. As shown in this figure, the ground surface acceleration time history is predominated by upward spiky acceleration whereas the acceleration time history at a depth of 260m does not show asymmetric nature.

The ground condition was idealized based on the P- and S-wave velocity profile shown in Fig. 10. The power index of n_K=0.5 was used for accounting the confining pressure dependency of stiffness within each layer. Further details can be found in a reference (Tobita et al., 2010). The soil deposit was initially subject to gravity and then subject to the input acceleration recorded at a depth of 260m with a peak acceleration of 0.7g for dynamic analysis. The effect of gravity is kept the same during the dynamic analysis. The computed acceleration time history at the ground surface is shown in the first row in Fig. 9. The computed acceleration time history shows spikes directed upward in the similar manner as recorded during the earthquake.

The analysis, shown in Fig. 11, basically supports the understanding of the mechanism of the strong asymmetric vertical motion described earlier: the mechanism is due to the nonlinear volumetric stress strain relationship of the soil discussed earlier. Dry soil cannot resist the tensile stress when the mass of subsurface soil is thrown upward (points “3” through “4” in Fig. 11) whereas there is a sudden recovery of compressive stress when the soil mass comes back to push the earth along with the downward motion (point “5” in Fig.11). Similarly to the idealized soil deposit subject to cyclic vertical acceleration discussed earlier, the spike is associated with the stress strain curve of a hard spring type for volumetric mechanism in the field during earthquakes.

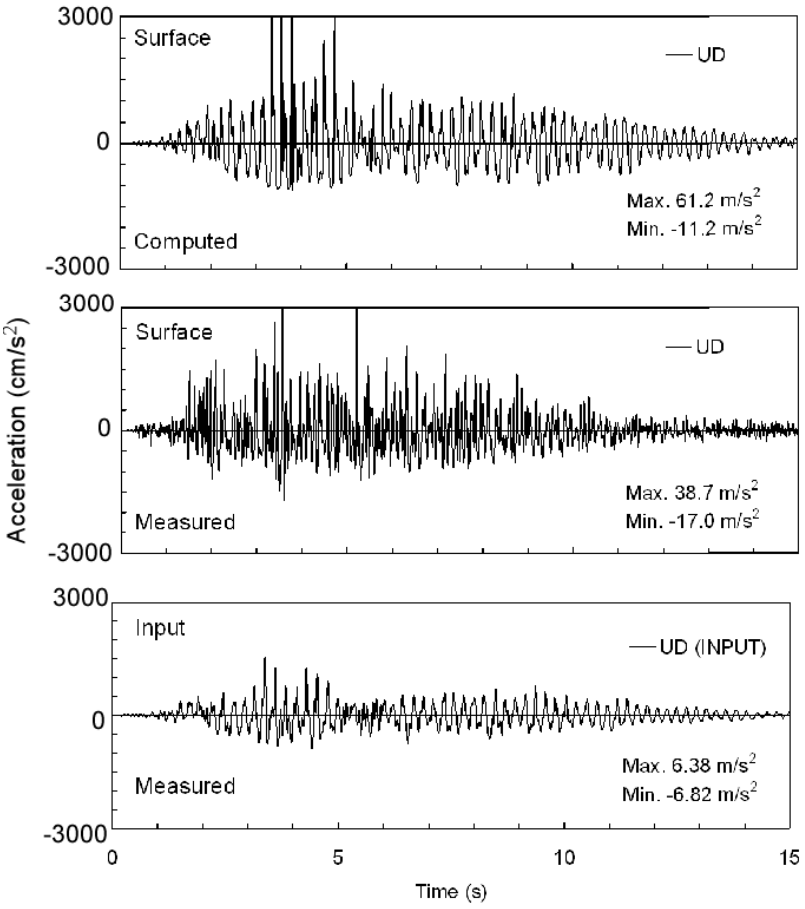

Fig. 9 Measured and computed acceleration at Ichinoseki-west, Japan, during the 2008 Iwate-Miyagi inland earthquake

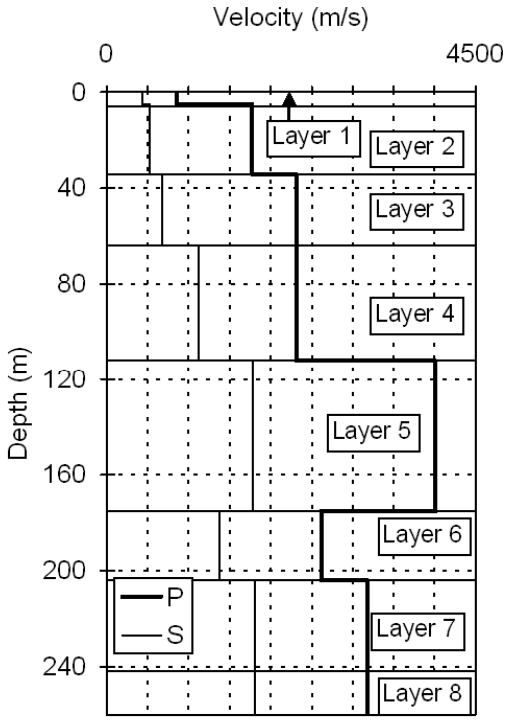

Fig. 10 P- and S-wave velocity profile at IWTH25 station

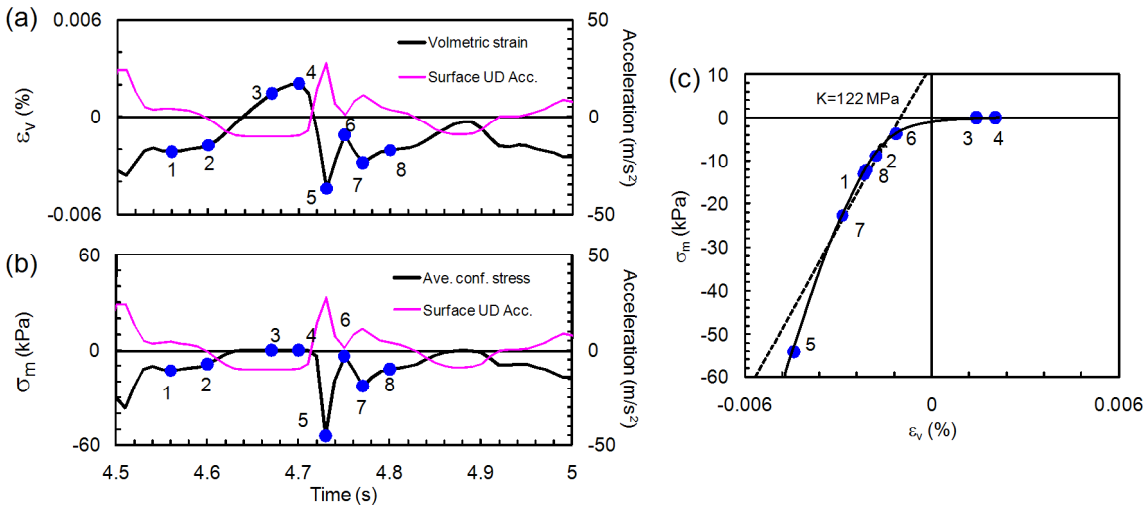

Fig. 11 Computed time histories from 4.5 to 5.0 (s); (a) volumetric strain, (b) mean stress. In (a) and (b), computed UD components of surface acceleration are plotted as a reference. (c) Mean stress versus volumetric strain relationship.

MECHANISM OF SPIKES IN SITE RESPONSE

Although the volumetric mechanism of soil is completely different from the shear mechanism, the spikes induced by the soil nonlinearity for volumetric and shear mechanisms have common element among them. As shown in the previous study (Iai et al., 1995; Iai and Tobita, 2006), the spikes in the horizontal component of acceleration time histories during liquefaction and cyclic mobility are associated with the stress strain curve for shear with a hard spring type. The hard spring type is associated with the recovery of the shear resistance as shear strain is induced. The dilatancy of soil is the primary mechanism for this. Figures 12 through 14 are reproduced from the previous papers as a backup to the discussions on nonlinearity in shear mechanism. As shown in Fig. 14 right, the stress strain curve for shear exhibits the hard spring type regime. The spikes shown in Figs. 12 and 13 at the ground surface (NS component) are associated with this hard spring type regime. Thus, when the mechanism of nonlinearity involves a hard spring type either in volume or shear mechanism, nonlinear site response tends to include the spiky response in acceleration.

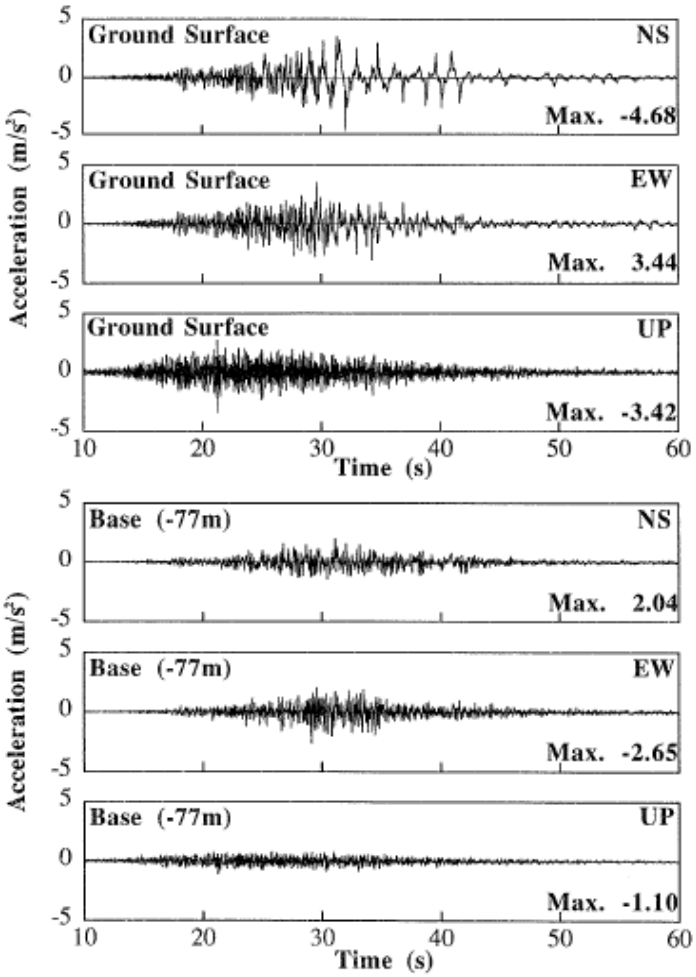

Fig. 12 Bore hole array data at Kushiro Port, Japan, during the 1993 Kushiro-Oki earthquake

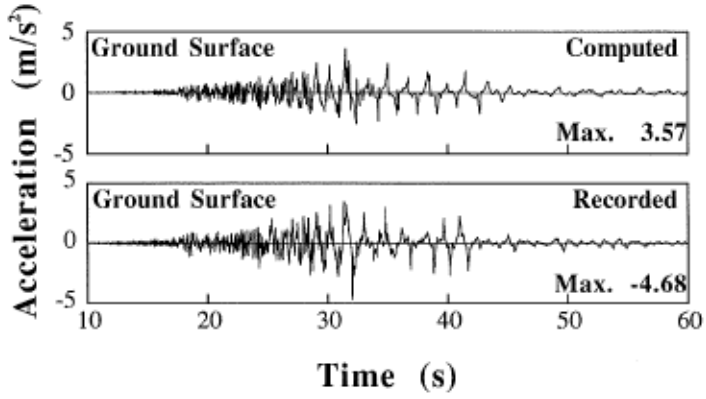

Fig. 13 Computed and recorded earthquake motions at ground surface at Kushiro Port, Japan

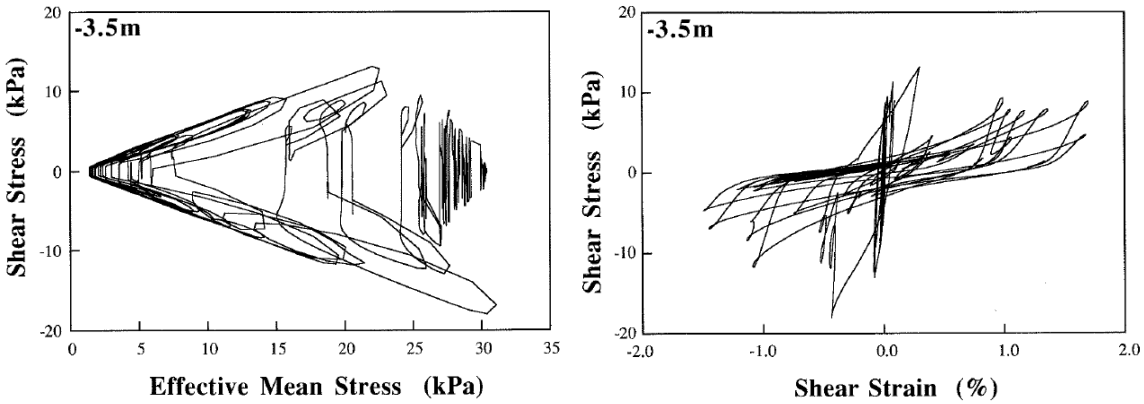

Fig. 14 Computed stress-strain behavior of soil (left: effective stress path, right: stress strain curve)

The discussions on the cause of the spikes due to a hard spring type material can be generalized as follows. In the case of a linear material, the response of the system does not change the frequency component of the input motion; the system only causes amplification or de-amplification in terms of amplitude and phase difference. In the case of a yielding spring type material, the system causes an elongation in terms of predominant period with tendency toward peak-cut or de-amplification and phase difference. The effect of a hard spring type material is considered just the opposite to the effect by the yielding spring type material. The hard spring type material tends to shorten 'the period' of predominant portion of each half wave with amplified peak value as shown in Figs. 6 through 8. The extreme case is the site response in the form of the spiky wave form as shown in Fig. 8 where 'the period' of predominant portion of each half wave approaches zero with a peak approaching infinity. Figure 15 schematically shows these response characteristics of a system depending on the types of the nonlinearity.

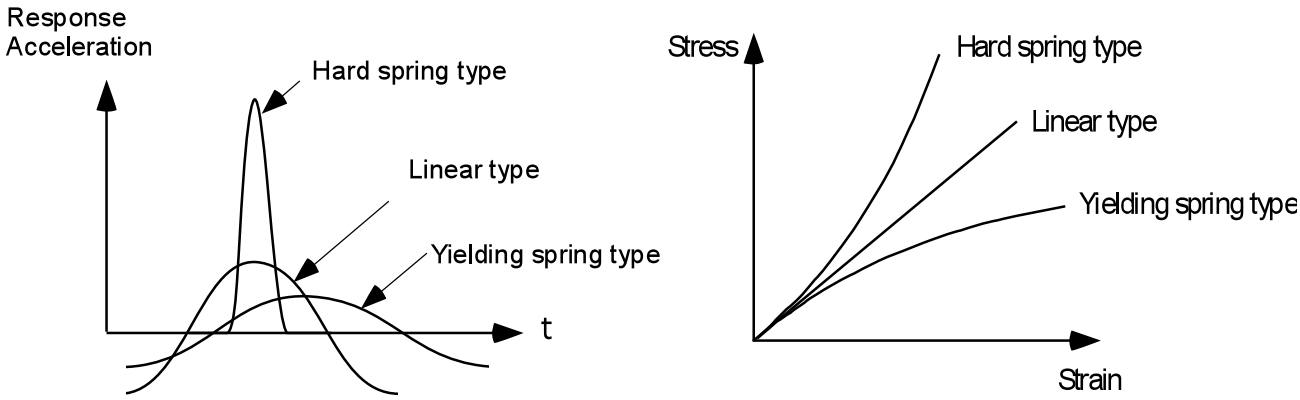

Fig. 15 Schematic figure of response of a system with various spring types subject to sinusoidal input motion

CONCLUSIONS

In this paper, nonlinearity due to volumetric mechanism is reviewed with the recently recorded asymmetric vertical motion with a peak acceleration of 4.0g during the 2008 Iwate-Miyagi Inland, Japan, earthquake. In the field, gravity provides static compression stress in the soil. When subjected to a vertical motion, the confining pressure may increase or decrease depending on the change in volumetric strain induced by the vertical motion. When the motion is small, the mechanism may be approximated by a linear volumetric mechanism. However, when the motion becomes sufficiently large, the change in the confining pressure will cause volumetric strain beyond the limit where there will be no compressible stress.

Dry soil tends to resist compression stress because contact forces between soil particles are mobilized during compression. However, when the dry soil is subject to tension, volumetric stretching (expansive) strain will be mobilized and eventually the soil particles will lose contacts among themselves with no isotropic stress mobilized in the soil. In this manner, the dry soil can exhibit nonlinear volumetric mechanism during earthquakes. The analysis based on the formulation of multiple mechanism model as proposed by the authors confirms that the asymmetric vertical motion with a peak acceleration of 4.0g recorded during the 2008 Iwate-Miyagi Inland, Japan, earthquake is indeed the results of nonlinearity in volumetric mechanism.

REFERENCES

Aoi, S., Kunugi, T. & Fujiwara, H. (2008). "Trampoline effect in extreme ground motion," *Science,* 322, 727-730.

Dobry, R. & Iai, S. (2000). "Recent developmnets in the understanding of earthquake site response and associated seismic code implementation," *GeoEng2000, An International Conference on Geotechnical & Geological Engineering,* Melbourne, Australia, 186-29.

Iai, S. (1993). "Micromechanical background to a strain space multiple mechanism model for sand," *Soils and Foundations,* 33(1), 102-117.

Iai, S., Morita, T., Kameoka, T., Matsunaga, Y. & Abiko, K. (1995). "Response of a dense sand deposit during 1993 Kushiro-Oki earthquake," *Soils and Foundations,* 35(1), 115-131.

Iai, S. & Tobita, T. (2006). "Soil non-linearity and effects on seismic site response," *Proc. 3rd International Symposium on the Effects of Surface Geology on Seismic Motion,* Grenoble, France, 21-46.

NEHRP (1997) *Recommended provisions for seismic regulations for new buildings and other structures*, Building Seismic Safety Council (BSSC), FEMA 203/303, Part 1 (Provisions) and Part 2 (Commentary)

Oda, M. (1974). "A mechanical and statistical model of granular material," *Soils and Foundations,* 14(1), 13-27.

Oda, M., Nemat-Nasser, S. & Konishi, J. (1985). "Stress-induced anisotropy in granular masses," *Soils and Foundations,* 25(3), 85-97.

Schnabel, P.B., Lysmer, J. & Seed, H.B. (1972) "*SHAKE A Computer program for earthquake response analysis of horizontally layered sites,"* Berkeley, University of California, Berkeley, Report No. EERC72-12.

Seed, H.B. & Idriss, I.M. (1970) "*Soil moduli and damping factors for dynamic response analyses,"* Berkeley, University of California, Berkeley, Report No. EERC70-10.

Sugito, M., Goda, H. & Masuda, T. (1994). "Frequency dependent equi-linearized technique for seismic response analysis of multi-layered ground," *Journal of Geotechnical Engineering, JSCE,* 493(III-27), 49-58 (in Japanese).

Terzaghi, K. (1943) *Theoretical Soil Mechanics,* New York, John Wiley and Sons, 510.

Tobita, T., Iai, S. & Iwata, T. (2010). "Numerical Analysis of Near-Field Asymmetric Vertical Motion," *Bulletin of the Seismological Society of America,* 100(4), 1456 - 1469.

Yoshida, N. & Iai, S. (1998). "Nonlinear site response and its evaluation and prediction," IN Irikura, K., Kudo, K., Okada, K. & Sasatani, T. (Eds.) *The Second International Symposium on the Effects of Surface Geology on Seismic Motion,* Yokohama, Japan, A.A.Balkema, 71-90.

Zeghal, M., Elgamal, A.W., Tang, H.T. & Stepp, J.C. (1995). "Lotung donwhole array. II: evaluation of soil nonlinear properties," *Journal of Geotechnical Engineering, ASCE,* 121(4), 363-378.